ARO 15882.13-M

LEVEL II

12

B.S.

AD A083546

Department of
Theoretical and Applied Mechanics
CORNELL UNIVERSITY
ITHACA, NEW YORK

(12)

(6) MATHEMATICAL THEORY OF LAMINAR COMBUSTION, VII. Cylindirical and Spherical Premixed Flames.

(9) Technical Report No. 109

(10) J.D. Buckmaster & G.S.S. Ludford

(11) March 1980

(12) 32

(14) TR-109

U.S. Army Research Office
Research Triangle Park, NC 27709

(15) Contract No. DAAG29-79-C-0121

Cornell University
Ithaca, NY 14853

Approved for public release; distribution unlimited

The findings of this report are not to be construed as an official Department of the Army position unless so designated by other authorized documents.

Foreward

This report is Chapter VII of the twelve in a forthcoming research monograph on the mathematical theory of laminar combustion. Chapter I-IV originally appeared as Technical Reports Nos. 77, 80, 82 & 85; these were later extensively revised and then issued as Technical Summary Reports No's 1803, 1818, 1819 & 1888 of the Mathematics Research Center, University of Wisconsin-Madison. References to I-IV mean the MRC reports

Contents

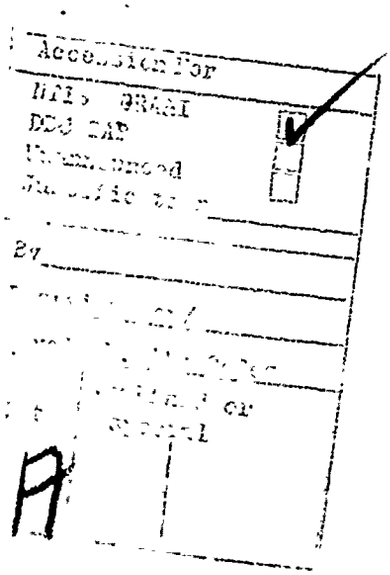

Chapter VII

Cylindrical and Spherical Premixed Flames

1. Cylindrical Flames

Although it has not been studied to the same extent as the plane premixed flame, the cylindrical flame is in principle almost as easy to produce. The reacting mixture is supplied through the surface of a circular cylinder and is induced to flow radially by means of sufficiently close end plates. The flame then forms a coaxial cylinder and can be observed through the end plates, which should be transparent and good thermal insulators.

Analytically the cylindrical flame stands between the plane and spherical flames. The structure of its reaction zone is the same as that of the plane flame, with temperature constant beyond; so that there is no curvature effect as for the spherical flame. On the other hand, like the spherical flame it does not exhibit the cold-boundary difficulty: the mixture must be introduced at a finite radius, which can however be so small that a line source is effectively formed. Ironically enough, in their attempt to treat curved flames Spalding & Jain (1959) use plane-flame analysis on the spherical flame, where it is never valid, and neglect the cylindrical flame, where it is always valid. ~~Ironically enough,~~ The results are qualitatively correct, however (Ludford, 1976).

The object of Secs. 2 & 3 is to show how cylindrical geometry modifies a premixed flame (Ludford 1980). For simplicity we shall consider a single reactant (monopropellant) undergoing a first-order reaction and take $\nu = 1$. Spherical premixed flames, which have many similarities to spherical diffusion flames, will be treated in Secs. 4-6.

2. Planar Character

We shall only consider the basic features of cylindrical flames; the discussion can easily be extended to other questions treated for plane flames in Chs. II & III. When making comparisons with the latter bear in mind that the non-dimensionalization is here based on the radius, a, of the supply cylinder.

If v is the radial velocity, the equation of continuity admits $r\rho v$ being constant. When M is the mass flux at the supply cylinder we may therefore write

$$r\rho v = M \quad \text{or} \quad \rho v = M/r, \tag{1}$$

the latter giving the mass flux at every other radius r. Once the temperature T has been determined, the density $\rho = 1/T$ and $v = MT/r$ follow immediately, while the small variations in pressure about its constant level can be calculated from the momentum equation of the mixture. There remain then the energy and reactant species equations

$$\mathcal{L}(Y) = -\mathcal{L}(T) = DY \exp(-\theta/T), \tag{2}$$

where

$$\mathcal{L} \equiv \frac{1}{r}\frac{d}{dr}\left(r \frac{d}{dr}\right) - \frac{M}{r}\frac{d}{dr} \tag{3}$$

in the cylindrical geometry.

First note that the Shvab-Zeldovich variable $\tilde{Y} = Y + T$ satisfies

$$\mathcal{L}(\tilde{Y}) = 0 \quad \text{for} \quad 1 < r < \infty. \tag{4}$$

Since the only solutions which remain bounded at infinity are constants, we have

(5) $$Y + T = T_\infty = Y_s + T_s$$

for a reaction that goes to completion, where s denotes conditions at the supply $r = 1$. The fact that the Y, T-relation is identical ~~that~~ to that for plane flames (Sec. II.2) is responsible for the structures of the reaction zones being the same.

The asymptotic analysis of the equations (2) proceeds as for a plane flame. The temperature beyond the flame sheet must be constant, i.e.

(6) $$Y = 0,\ T = T_\infty \quad \text{for} \quad r > r_*,$$

while up to the flame sheet the reaction is frozen, i.e. $\mathcal{L}(Y) = \mathcal{L}(T) = 0$, so that

(7) $$Y = Y_s + L(1 - r^M),\ T = T_s + L(r^M - 1) \quad \text{for} \quad 1 < r < r_*.$$

Here $L = M^{-1}T_s'$, with T_s' the temperature gradient at the supply, is the heat conducted back into the supply per unit mass of mixture. These two pairs of formulas (6), (7) give the same values at

(8) $$r_* = [1 + (T_\infty - T_s)/L]^{1/M};$$

as expected, the stand-off distance for a plane flame is recovered as the radius a of the supply cylinder tends to infinity when due attention is paid to a mass-flux unit proportional to $1/a$. Consistency requires $r_* > 1$, i.e.

(9) $$L > 0,$$

which means the supply must be a conductive heat sink.

As before the interior of the flame sheet is investigated with the expansions

(10) $$Y = \delta y(\xi) + o(\delta),\ T = T_\infty + \delta t(\xi) + o(\delta)$$

where

(11) $\xi = (r - r_*)/\delta$ and $\delta = T_\infty^2/\theta$.

The structure is thereby found to satisfy the equation

(12) $d^2t/d\xi^2 = -\tilde{D}\, y\, e^t$, where $y + t = 0$,

and the boundary conditions

(13) $t = MJ_s\xi/r_* + o(1)$ as $\xi \to -\infty$, $t = o(1)$ as $\xi \to +\infty$,

which come from matching with the expressions (6) and (7) outside. Here

(14) $\tilde{D} = \delta^2 e^{-\theta/T_\infty} D$ while $J_s = Y_s - Y_s'/M$

is the reactant flux fraction $Y - rY'/M$ at the supply (usually 1). Exactly the same problem is obtained for a plane flame except that the coefficient MJ_s/r_* in the condition (13a) is replaced by MJ_* (which equals MJ_s there). Noting that here $J_* = J_s/r_*$ (because the total reactant flux $2\pi rMJ$ is conserved for frozen chemistry) shows that the cylindrical reaction zone is locally plane. For spherical flames the y,t-relation (12b), which derives from the Y,T-relation (5) is changed; so that the reaction zone is quite different from its plane counterpart.

From the solution (II.21) of the corresponding plane-flame problem we deduce

(15) $\tilde{D} = (J_s/r_*)^2 M^2/2$

so that

(16) $D = (J_s^2\theta^2 e^{\theta/T_\infty}/2T_\infty^4 r_*^2)M^2$,

which is the required M,D-relation. (The presence of r_* in this formula means that it depends on all supply parameters, unlike the plane flame.) For fixed

ML, i.e. heat conducted back to the supply, it has the general shape of the parabola (II.22) obtained for the plane flame, because the factor

$$1/r_*^2 = [1 + (T_\infty - T_s)/L]^{-2/M} \tag{17}$$

varies only between $\exp[-2(T_\infty - T_s)/ML]$ and 1 as M increases from 0 to ∞. The parabola is useful for determining the speed (i.e. M) with which a plane flame propagates into fresh mixture at given pressure (i.e. D), but there is no equivalent use here. On the other hand, for the set-up envisaged in the opening paragraph both M and D are prescribed (along with T_s and J_s), and the formula determines the final temperature T_∞ (note $L = J_s + T_s - T$).

3. Near-Surface and Surface Flames. Remote Flames.

For the above solution to be valid the parameter values must be such that r_*, as given by the formula (8), lies between 1 and ∞ . As for the plane flame (Sec. II.5) three limiting cases arise, two of which are essentially the same as there. The third leads to an interesting new phenomenon.

When M and D become large, with all other parameters held fixed, the flame approaches the surface. An intense convective-diffusive zone of thickness $O(M^{-1})$ forms near the surface, bounded by a reaction zone whose thickness is $O(\theta^{-1}M^{-1})$.

By contrast a true surface flame can be produced for any M by adjusting the pressure so as to make $T_\infty \to T_s$. Similarly remote flames can be produced by making $T_\infty \to J_s + T_s$ (i.e. $L \to 0$). At both extremes the preceding analysis becomes invalid: either the boundary intrudes into the reaction zone and there is no frozen region between them or the isothermal limit of (7) is not uniformly valid in the unbounded frozen region. In either case the asymptotics must be reworked.

The analysis of the surface flame is identical ~~that~~ to that for the plane case provided x is changed to $r-1$. We conclude that $\tilde{D}$ will change from $J_s^2 M^2/2$, the value (15) when $r_* = 1$, to ∞ as the temperature difference $T_\infty - T_s$, measured on the δ-scale, decreases from ∞ to 0.

By contrast, the remote flame cannot be treated as in the plane case since the asymptotic analysis breaks down earlier, in fact as soon as L becomes $O(\delta)$. The difference lies in the reactant flux $M J_s/r_*$ at the flame, which now tends to zero like $\delta^{1/M}$ as $r_* \to \infty$; the condition (13a) loses its effectiveness unless a different scale is used for the structure. Setting

$$r = r_* + \delta^{1-1/M}\xi \tag{18}$$

gives the new condition

$$t = MJ_s(\ell/J_s)^{1/M}\xi + o(1) \quad \text{as } \xi \to -\infty. \tag{19}$$

where $L = \delta\ell$; the corresponding change

$$\tilde{D} = \delta^{2(1-1/M)}\, e^{-\theta/T_\infty} D \tag{20}$$

must also be made to keep the structure equation balanced.

We therefore end with the same problem, except that r_* is replaced by $(J_s/\ell)^{1/M}$; so that $\tilde{D}$ is given by the formula (15) with the same replacement and

$$D = J_s^{2(1-1/M)}\, \theta^{2(1-1/M)}\, e^{\theta/T_\infty} \ell^{2/M}/2T_\infty^{4(1-1/M)}. \tag{21}$$

Thus D varies from 0 to ∞ on the scale $\theta^{2(1-1/M)}\, e^{\theta/T_\infty}$ as ℓ increases from 0 to ∞, the upper end of the range corresponding to 0 on the previous scale $\theta^2 e^{\theta/T_\infty}$.

The most interesting feature is the spreading of the zone in which there is chemical activity, as M decreases. The transformation (18) implies that its

thickness is $O(\theta^{1/M-1})$, so that for $M \leq 1$ it is no longer a sheet; indeed for $M < 1$ it has infinite extent [remember $r_* = O(\theta^{1/M})$ is larger still]. Such a phenomenon should be easily observable.

We have ssen that, except when remote, the cylindrical flame is locally plane, unlike the spherical flame. These results stem from the diffusion-convection operator

$$\mathcal{L} \equiv \frac{1}{r^\alpha}\left[\frac{\partial}{\partial r}\left(r^\alpha \frac{\partial}{\partial r}\right) - M\frac{\partial}{\partial r}\right] \tag{22}$$

governing the reactionless field behind the flame. Here $\alpha = 0$ (plane, when $r = x$), 1 (cylindrical) or 2 (spherical) and

$$\mathcal{L}(T) = 0 \tag{23}$$

has the general solution

$$T = A + B\,e^{Mr} \quad (\alpha = 0), \quad A + B\,r^M \quad (\alpha = 1), \quad A + B\,e^{-M/r} \quad (\alpha = 2) \tag{24}$$

in the three cases. Boundedness of T makes $B = 0$ in the first two cases but not in the third, where T_∞ becomes an assignable parameter in addition to any others. It is this difference between the convection-diffusion process in plane and cylindrical geometries on the one hand and spherical geometry on the other which accounts for the similarities and differences of the corresponding flames.

4. Spherical Flames. Damköhler-Number Asymptotics.

If general values of ν_1 and ν_2 had been retained in Ch. VI, most of the remaining results in the present chapter could now be obtained by setting $\nu_1 = 0$, $\nu_2 = 1$ i.e. $\alpha_1 = 0$, $\alpha_2 = -1$ (cf. Normandia & Ludford 1980). The exceptions concern strong burning with $M \to \infty$. However, the analysis need only be

sketched, omitted details being similar to those in Ch. VI.

We shall suppose that

(25) $$T_s \quad \text{and} \quad M^{-1}T_s' = L$$

are prescribed at the supply and that

(26) $$J_s \equiv Y_s - M^{-1}Y_s'/\mathcal{L} = 1$$

there (so that it is purely a source of reactant). Prescribing T_∞ and requiring

(27) $$Y_\infty = 0$$

then places five boundary conditions on the fourth-order system (VI. 2,3) for T and Y, so that we may expect M to be determined by D.

Consider steady states and take $\mathcal{L} = 1$. Then the mixture velocity is given by equation (VI.6) and the single variable Shvab-Zeldovich is

(28) $$H \equiv T + Y = T_\infty + (T_a - T_\infty)(1 - e^{-M/r}),$$

where

(29) $$T_a = T_s - L + 1$$

is the adiabatic flame temperature. The problem again reduces to one for T alone, namely

(30) $$\mathcal{L}(T) = -DYe^{-\theta/T} \quad \text{for} \quad 1 < r < \infty \text{ with } T_s, L \text{ and } T_\infty \text{ prescribed.}$$

Its comprehensive treatment is due to Ludford, Yannitell & Buckmaster (1976a,b); the most important features were simultaneously found by Liñán (1975).

We first turn to the limits $D \to 0, \infty$, which had already been considered by Fendell (1969). Frozen combustion is described by the same formulas as for the diffusion flame, provided the new definition

$$\varepsilon = De^{-\theta/T_\infty} \tag{31}$$

is made; in particular the burning rate (VI.11) holds. Equilibrium limits ($D \to \infty$) require

$$Y = 0 \tag{32}$$

outside the reaction zone, a state that cannot hold next to the source: the zone must therefore lie on the surface of the source. There are two possibilities, according as M is finite or not; the former is the counterpart of the surface diffusion flame and the latter corresponds to the Burke-Schumann flame, as we shall now see.

If general stoichiometric coefficients had been retained, the formulas (VI. 14, 15) would have had $-Z_\infty/2\alpha_2$ in place of Z_∞. Then $M_e \to \infty$ and $r_* \to 1$ as $\alpha_2 \to 0$: the Burke-Schumann solution tends to a surface flame with indefinitely large burning rate as the oxidant becomes inactive. The limit behavior cannot be deduced from generalizations of the expansions (VI. 17,18,19) but must be determined ab initio.

For that purpose, note that the Shvab-Zeldovich relation (28) gives

$$T = T_a \quad \text{for} \quad r > 1 \tag{33}$$

with an adjustment to T_∞ at distances $O(M)$. The temperature must therefore vary to leading order in the reaction zone; as also follows from the boundary condition $M^{-1}T_s' = L$, which in addition points to

$$x = M(r-1) \tag{34}$$

as the appropriate coordinate there. We conclude that the reaction zone is governed by

$$(35) \qquad (d^2/dx^2 - d/dx)T = DM^{-2}Y\exp(-\theta/T),\ Y + T = T_a,$$

$$(36) \qquad T = T_s,\ dT/dx = L \quad \text{for} \quad x = 0 \quad \text{and} \quad T \to T_a \quad \text{as} \quad x \to \infty,$$

i.e. the plane problem for a vaporizing liquid considered in Sec. II.3. It follows that

$$(37) \qquad DM^{-2} = \Lambda(T_s, L, \theta),$$

where Λ is the eigenvalue introduced there, determines how M tends to infinity with D.

The asymptotic form (II.22) of Λ as $\theta \to \infty$ was the goal of Sec. II.4, its determination for finite θ being a numerical question on which a great deal of effort has been spent in the past. For the diffusion flame the Burke-Schumann solution can be written in simple analytical terms for any θ, but here we end with the corresponding plane problem. Even the asymptotic behavior of M, the counterpart of the formula (VI.14), is a numerical question. One simple feature does remain, however: the plane solution only exists for

$$(38) \qquad L < 1$$

[a limiting form of the condition (VI.20)], as was shown in Sec. II.4.

We turn now to the equilibrium limit which is the counterpart of the surface diffusion flame; for convenience we shall refer to it as the Buckmaster limit also. M remains finite, the temperature is constant to leading order in the reaction zone and the Shvab-Zeldovich relation (28) gives

$$(39) \qquad M = M_s \equiv \ell n[1 + (T_\infty - T_s)/(L-1)]$$

in place of the result (VI.21). The expansions (VI.22,23) are replaced by

$$M = M_s[1 + D_*^{-1/2}/(1-L) + o(D_*^{-1/2})] \tag{40}$$

and

$$T = T_s + D_*^{-1/2}M_s[1 - e^{-\xi} + (L-1)\xi] + o(D_*^{-1/2}) \tag{41}$$

if the new definition

$$D_* = De^{-\theta/T_s} \tag{42}$$

is made. The changes amount to 2 being replaced by 1 to account for the different (non-dimensional) heat release at the flame. Restrictions on the parameters come from M_s, which must be positive if the (small) mass fraction of reactant is to be positive:

$$T_\infty \gtrless T_s \quad \text{according as} \quad L \gtrless 1. \tag{43}$$

The conditions for the existence of the three limits determine three regions in the parameter plane (Fig. 1) in each of which two of the limits hold. In the fourth region there is no solution for any values of D and θ: the Shvab-Zeldovich relation (28) would require Y_s to be negative there.

5. Ignition and Extinction.

We turn now to activation-energy asymptotics, starting with the nearly adiabatic flame for $\mathcal{L} \neq 1$, i.e. the analog of Sec. VI.3. Again, different values of k in the defining condition (VI.[illegible]) will be generated by varying T_s keeping T_∞ and L fixed with

$$L < 1. \tag{44}$$

The frozen and infinite-M limits then exist.

Slow variations are governed by the analog

$$M(T_a - H_*) = \mathcal{J}(Y) - r_*^2(\partial T/\partial r + \mathcal{L}^{-1}\partial Y/\partial r)_* \tag{45}$$

of the result (VI.45), where now

$$\theta\mathcal{J}(Y) = \int_1^{r_*} r^2 \frac{\partial}{\partial \tau}[\rho(Y-H_*)]dr. \tag{46}$$

To use this formula the combustion field must be determined to appropriate accuracy. Noting that, as before, it is frozen ahead of the flame and in equilibrium behind we find

$$T = \begin{cases} T_s - L + Le^{M(1-1/r)} + o(1), \\ T_\infty + \theta^{-1}C(1-e^{-M/r}) + o(\theta^{-1}), \end{cases} \qquad Y = \begin{cases} 1 - e^{\mathcal{L}M(1/r_*-1/r)} + o(1) \text{ for } 1 < r < r_*, \\ 0 \text{ (to all orders) for } r_* < r < \infty, \end{cases} \tag{47}$$

where

$$r_* = M/(M + \ell n\ L), \tag{48}$$

as replacements for the results (VI.47,48,49,51). Substitution in the basic equation (45) yields the same results (VI.52), where now

$$b = \int_0^{\ell n(1/L)} \frac{(Le^{\ell})^{\mathcal{L}} - Le^{\ell}}{T_s - L + Le^{\ell}} \frac{d}{d\ell}\left[\frac{\ell}{(M-\ell)^4}\right]d\ell. \tag{49}$$

As before, a second relation between C and M comes from the structure, the analysis of which is very similar to that of the diffusion flame in Sec. VI.3. We find

$$C(1-e^{-M/r_*}) = T^2\ \ell n(M^2\theta^2 e^{\theta/T_\infty}/2D\mathcal{L}r_*^4\ T_\infty^4); \tag{50}$$

so that elimination of C yields the basic equation

$$(51) \qquad bM\,dM/d\tau = k - (1 - e^{-M/r_*})^{-1} T_\infty^2 \ell n(M^2\theta^2 e^{\theta/T_\infty}/2D\mathcal{L} r_*^4 T_\infty^4)$$

where $r_*(M)$ is the function (48). The steady-state response for $k = 0$ has a simple algebraic form in which D is proportional to $(M + \ell n\, L)^4/M^2$, a result essentially found by Fendell (1972). Otherwise the above analysis has not been published before.

Steady-state responses are shown in Fig. 2. They differ from those for the diffusion flame (Fig. VI.4) because of the factor $\mathcal{Z}_*$ there, which vanishes at the Burke-Schumann value (VI.64); here M tends to infinity (like $D^{1/2}$) on all curves. For large values of k the turning points are

$$(52) \qquad M \sim \ell n(1/L) + 4T_\infty^2/k, \quad D \sim (4/e)^4 T_\infty^4 \theta^2 e^{\theta/T_\infty}/2(\ell n\, L)^2 \mathcal{L} k^4$$

and

$$(53) \qquad M \sim \ell n(k/LT_\infty^2) + \ell n\, \ell n(k/LT_\infty^2) - \ell n\, 2,$$

$$(54) \qquad D \sim (\theta^2 e^{\theta/T_\infty}/2\mathcal{L} T_\infty^4)\,(M^2 + 4\,\ell n\, L\, M + 6\,\ell n^2 L).$$

Conditions for instability, predicted by the full equation (51) are the same as for the fuel drop: for $\mathcal{L} < 1$ the middle branch of an S-response is unstable; for $\mathcal{L} > 1$ the other two branches, as well as the whole of a monotonic curve, are unstable.

These results and those in the previous section suggest that an S-response will be obtained in the triangular region

$$(55) \qquad T_s < T_\infty < T_a$$

of the parameter plane (Fig. 1). The first inequality ensures that a weak-burning limit exists, while the second comes from the existence of such near-adiabatic responses for k sufficiently large. As for the diffusion

flame, the lower branch (including the ignition point) will be obtained for values M within $O(\theta^{-1})$ of its frozen value. A similar analysis cannot be made of the upper branch, however, because the Burke-Schumann limit is now infinite. The treatment required has been given by Kapila, Ludford & Buckmaster (1975).

Take $\mathcal{L} = 1$ again. At any point on the lower branch the temperature is still given by the formulas (VI.66,67). Moreover, at infinity the equation (VI.70) and boundary conditions (VI.71) still hold, provided only that

$$D_w = D\theta^{-2} e^{-\theta/T_\infty} \tag{56}$$

now. The lower branch is threfore given by Fig. VI.6 again, which may be used to read off the ignition point.

Although M goes to infinity in the equilibrium limit the combustion field for strong burning, i.e. M large but finite, has the same structure (35,36). In the limit $\theta \to \infty$ it shows a flame sheet located within $O(M^{-1})$ of the surface, with equlibrium beyond. (Since the decomposition zone has thickness $O(\theta^{-1})$ on the x-scale, it stands clear of the surface however large M is.) We therefore have the plane problem of Sec. II.4 except that the temperature is not constant behind the flame but varies according to equation (28) with Y = 0. As a consequence the flame temperature is perturbed away from T_a:

$$T_* = T_a + (T_\infty - T_a)e^{-M}/L. \tag{57}$$

The result (II.22), with $J_s = 1$ and T_∞ replaced by this T_*, gives the response curve

$$\tilde{D} = M^2 \exp(\tilde{\theta}e^{-M}) \tag{58}$$

to leading order, where

(59) $\tilde{D} = [2T_a^4\theta^{-2}\exp(-\theta/T_a)]D$ and $\tilde{\theta} = [(T_a-T_\infty)/LT_a^2]\theta$.

The response has a turning point at $M = M_e(\tilde{\theta})$ where

(60) $$e^{M_e} = (\tilde{\theta}/2)M_e,$$

i.e.

(61) $$M_e = \ell n(\tilde{\theta}/2) + \ell n\ell n(\tilde{\theta}/2) + o(1).$$

[Note that this result only makes sense if $\tilde{\theta} \to +\infty$, i.e. for $T_\infty < T_a$, as supposed.] Near the turning point we write

(62) $M = M_e + m$ with $m = O(1)$

to obtain

(63) $$\tilde{D} = M_e^2 + 2M_e(m + e^{-m}) + O(1).$$

The function $m + e^{-m}$ is graphed in Fig. 3. The results (61) and (63), with $m = 0$, are explicit asymptotic formulas for the location of the extinction point.

6. Other Aspects of Responses.

We shall now briefly describe the middle branch of the S-response, the two types of monotonic response (depending on the nature of the equilibrium limit) and the C-response. A detailed treatment of all these has been given by Ludford, Yannitell & Buckmaster (1976a,b), in particular for the C-response where there is no analogous discussion of spherical diffusion flames (Sec. VI.6).

The flame temperature on the middle branch, which ranges from T_∞ to T_a, is always the maximum temperature in the combustion field, so that the reaction is frozen on either side of the flame sheet. While there could still be

equilibrium to leading order beyond the flame, we shall first suppose that is not the case. As in Sec. VI.5 we shall consider M to be specified and anticipate the equal conduction of heat to the two sides of the flame. The temperature profiles (VI.89) still hold and lead to the results (VI.90,91) with the 2 deleted. The structure equation (VI.92) still governs, provided the new definition

$$D_m = D_o Y_* e^{-\theta/T_*} \tag{64}$$

is used. As for the diffusion flame, details of the determination of D_m are not needed to draw the conclusion (VI.95).

The bound (VI.96) shows that the solution holds for

$$T_\infty < T_a - 1/2 \tag{65}$$

now; there are clearly no paramter values for which it covers the whole range of M, since that is infinite here. Over the rest of the middle branch, i.e. the whole of it when the inequality (65) is not satisfied, T_* is zero and the complete-burning structure of the monotonic response is needed. Examples of computed S-responses are shown in Fig. 4.

We turn now to the monotonic responses, for which the inequality (VI.99) holds and the temperature increases beyond the flame sheet. The formulas (VI.100, 101, 102) are still valid, provided the 2 is deleted from the last two, so that dT_*/dM is again negative and D is again an increasing function of M to leading order. Once more the monotonicity of the response is established without discussing the flame-sheet structure. The latter is of course needed to construct the curves themselves (Fig. 5).

As M increases from its frozen value, r_* decreases from ∞ to 1 and there are two possibilities. If L is less than 1, so that the limit (39) does not exist, then M increases without bound with T_* approaching T_a as the flame sheet approaches the surface. The frozen limit is joined to the Burke-Schumann limit of infinitely rapid burning. If L is greater than 1, so that the limit (39) does exist, then T_* approaches T_s as the flame sheet settles down on the supply sphere. The frozen limit is joined to the Buckmaster limit, the approach to which is similar to that for diffusion flames (Sec. VI.6).

Finally we come to supplies that are hotter than the ambient atmosphere, i.e. inequality (VI. 106). The frozen limit does not exist but both equilibrium limits do. The response takes the shape of a C whose upper part always corresponds to complete burning but whose lower part may correspond to incomplete burning. The division (if it occurs) lies below the leftmost point of the C, which corresponds to both ignition and extinction conditions, so that these conditions are determined by the formulas (61,63). An example of such a response is shown in Fig. 6.

The application of the results in this chapter to the burning of monopropellant drops follows the same lines as Sec. VI.7. While we have restricted our attention to inert atmospheres, the problem of the ambient being an oxidizing atmosphere for the product of the decomposition should also be investigated. There is now a diffusion flame in addition to the premixed one, so that features from Ch. VI will also arise. The Damköhler-number asymptotics have already been considered by Fendell (1969) and, more completely, by Buckmaster, Kapila & Ludford (1978), but much remains to be done.

References

Buckmaster, J.D., Kapila, A.K. & Ludford, G.S.S., 1978, Monopropellant decomposition in a reactive atmosphere, Combust. Sci. Tech. 17, 227-236.

Fendell, F.E., 1969, Quasi-steady spherico-symmetric monopropellant decomposition in inert and reactive environments, Combust. Sci. Tech. 1, 131-145.

Fendell, F.E., 1972, Asymptotic analysis of premixed burning with large activation energy, J. Fluid Mech. 56, 81-95.

Kapila, A.K., Ludford, G.S.S. & Buckmaster, J.D., 1975, Ignition and extinction of a monopropellant droplet in an inert atmosphere, Combust. Flame 25, 361-368.

Liñán, A. 1974, The asymptotic structure of counterflow diffusion for large activation energy, Acta Astronaut. 1, 1007-1039.

Liñán, A., 1975, Monopropellant droplet decomposition for large activation energies, Acta Astronaut. 2, 1009-1029.

Ludford, G.S.S., 1976, Combustion for large activation energy, Letters Appl. Eng. Sci. 4, 49-61.

Ludford, G.S.S., 1980, Premixed cylindrical flames, Transactions of the 26th Conference of Army Mathematicians, Baltimore, MD. (ARO Rept.),

Ludford, G.S.S., Yannitell, D.W. & Buckmaster, J.D., 1976a, The decomposition of a cold monopropellant in an inert atmosphere, Combust. Sci. Tech. 14, 133-146.

Ludford, G.S.S. Yannitell, D.W. & Buckmaster, J.D., 1976b, The decomposition of a hot monopropellant in an inert atmosphere, Combust. Sci. Tech. 14, 125-131.

Normanida, M.J. & Ludford, G.S.S., 1980, Surface equilibrium in drop combustion, SIAM J. Appl. Math. 38,

Spalding, D.B. & Jain, V.K., 1959, Theory of the burning of monopropellant droplets, Aero. Res. Council Current Paper No. 447, Tech. Rept. 20, 176.

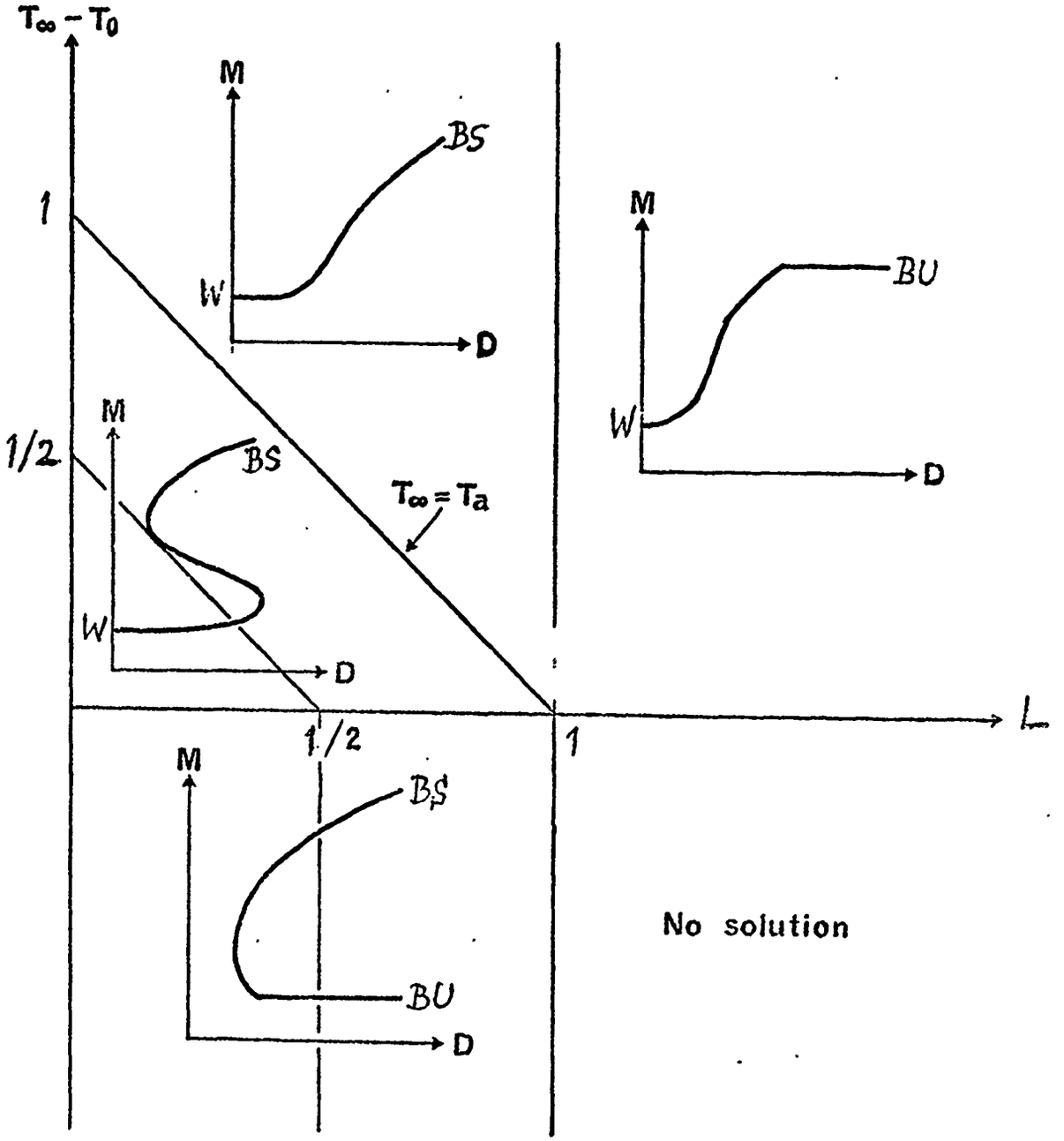

Fig. 1. Parameter plane showing responses:
W = weak-burning limit,
BS = Burke-Schumann equilibrium limit,
BU = Buckmaster equilibrium limit.

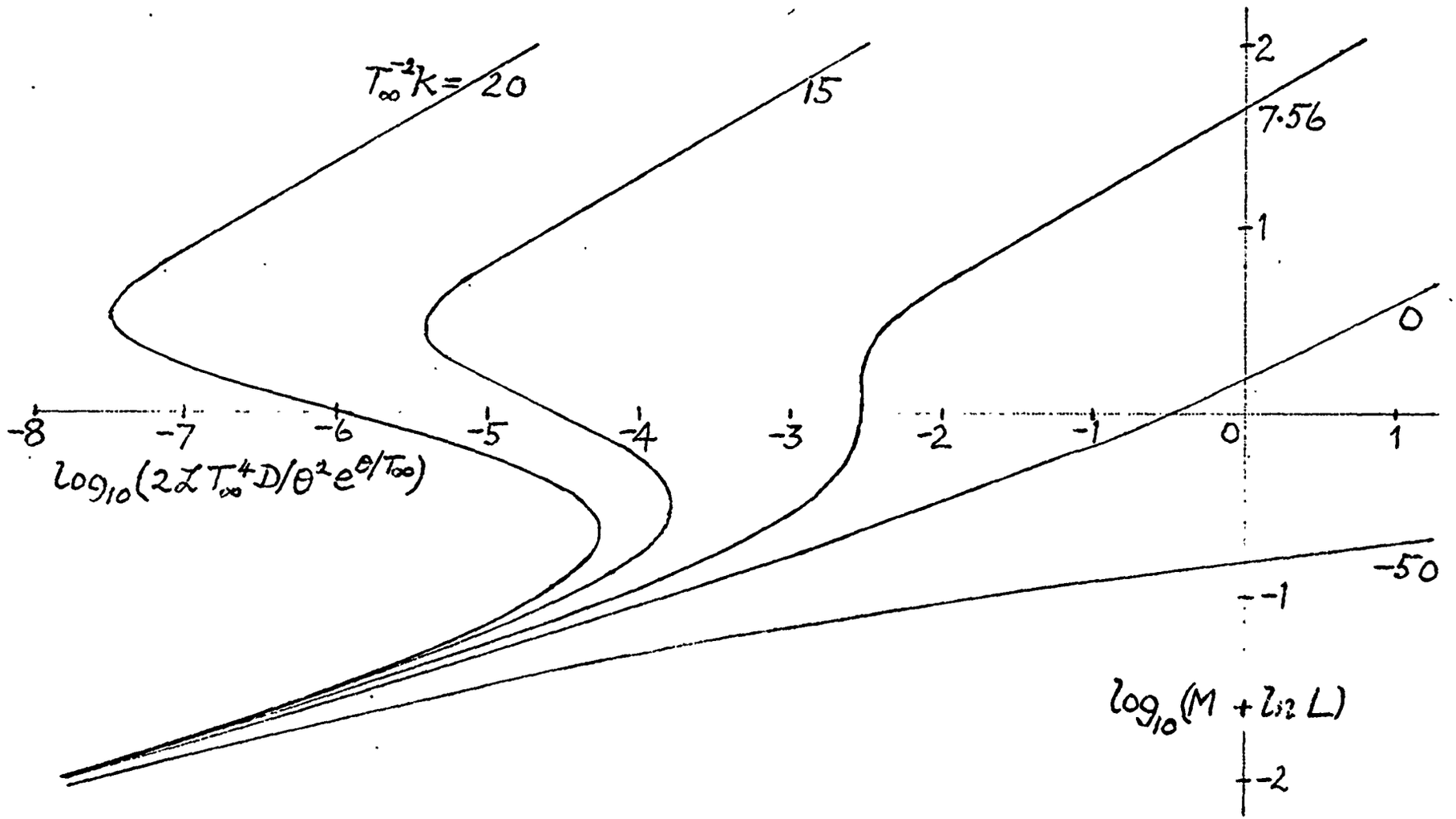

Fig. 2. Response of nearly adiabatic flame; drawn for $L = 0.5$.

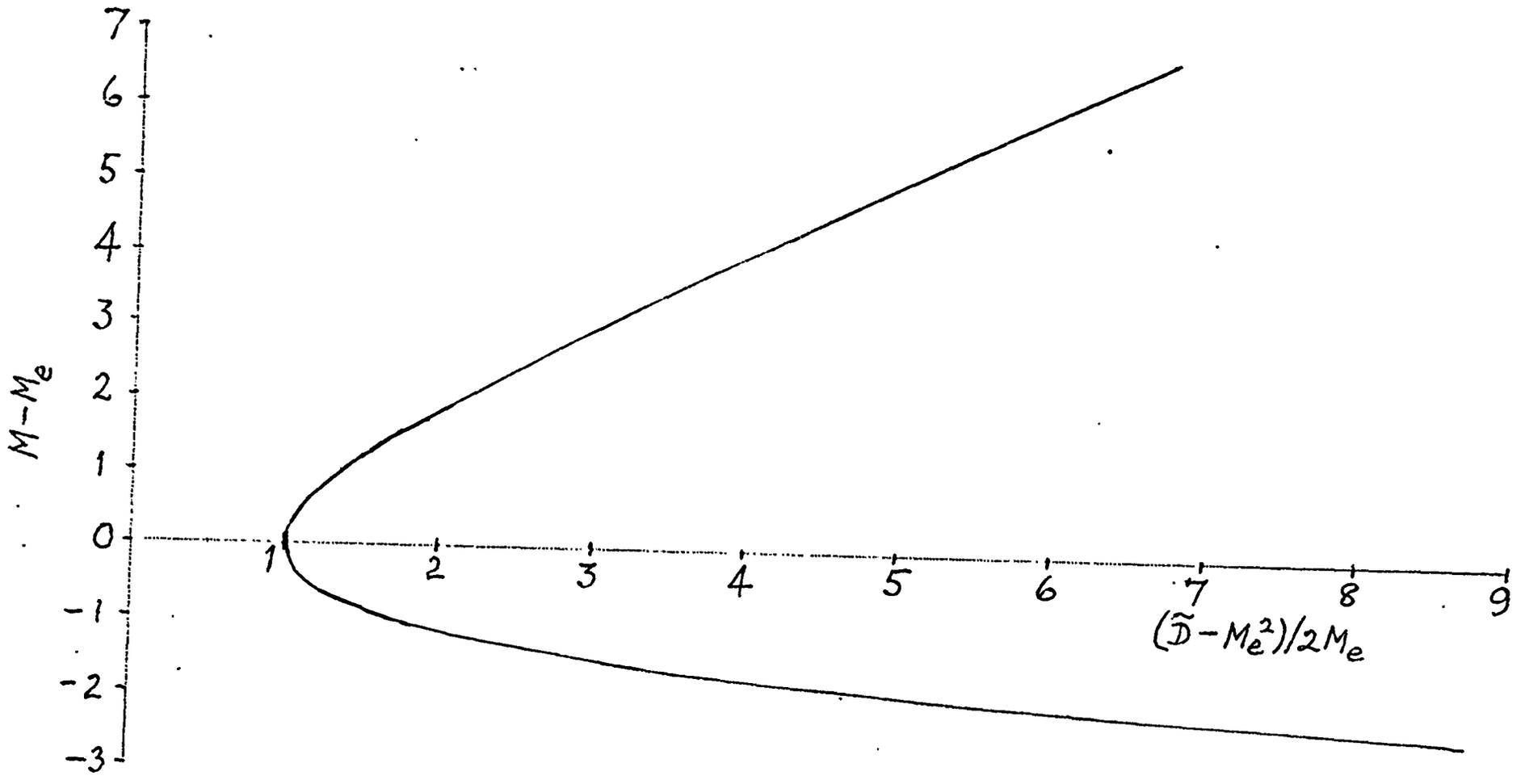

Fig. 3. Universal extinction curve: $M-M_e=m$, $(\tilde{D}-M_e^2)/2M_e=m+e^{-m}$.

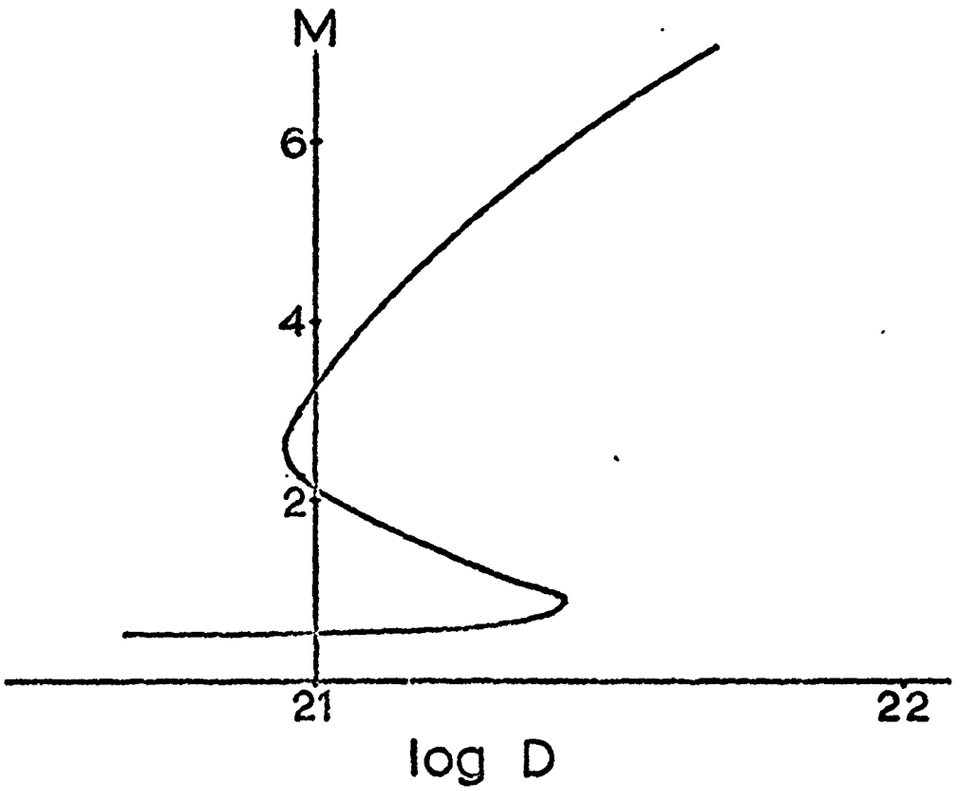

Fig.4. S-response for $\theta = 50$ and
a) $T_\infty = 1$, $T_s = 0.75$, $L = 0.5$.

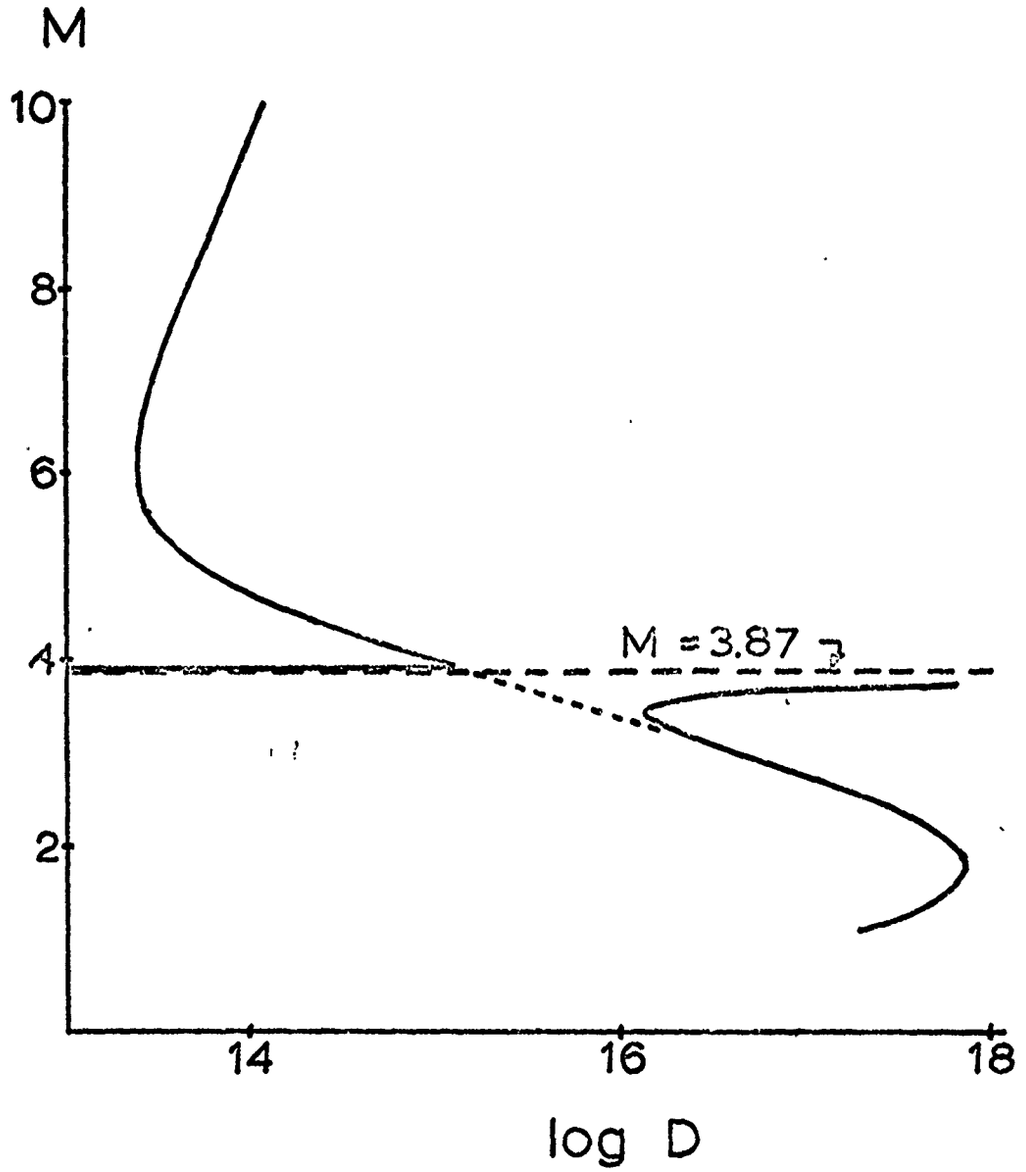

Fig. 4. S-response for $\theta = 50$ and
b) $T_\infty = 1$, $T_s = 0.98$, $L = 0.02$.

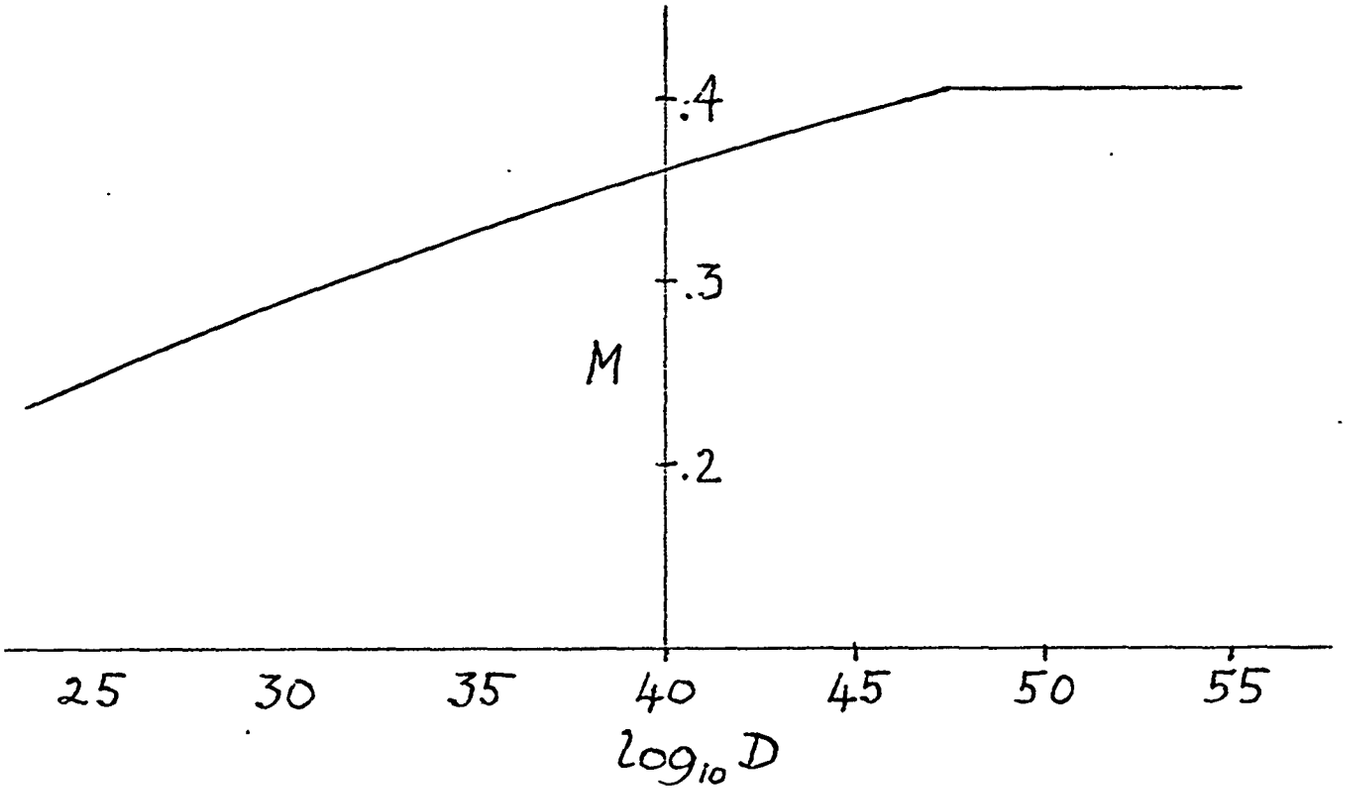

Fig.5. Monotonic response for $\theta = 50$ and a) $T_\infty = 1$, $T_s = 0.5$, $L = 2$.

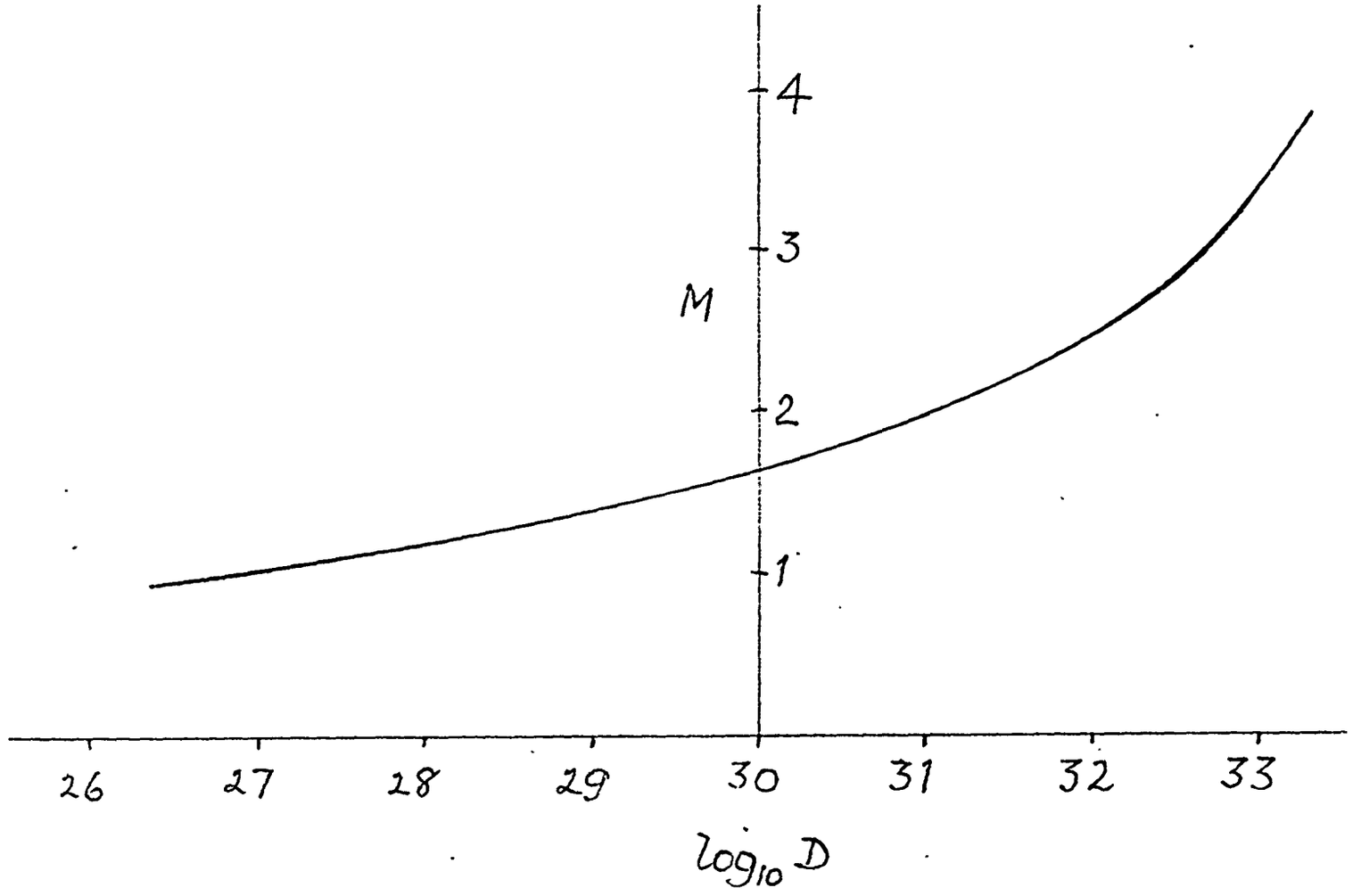

Fig.5. Monotonic response for $\theta = 50$ and
b) $T_\infty = 1$, $T_s = 0.5$, $L = 0.75$.

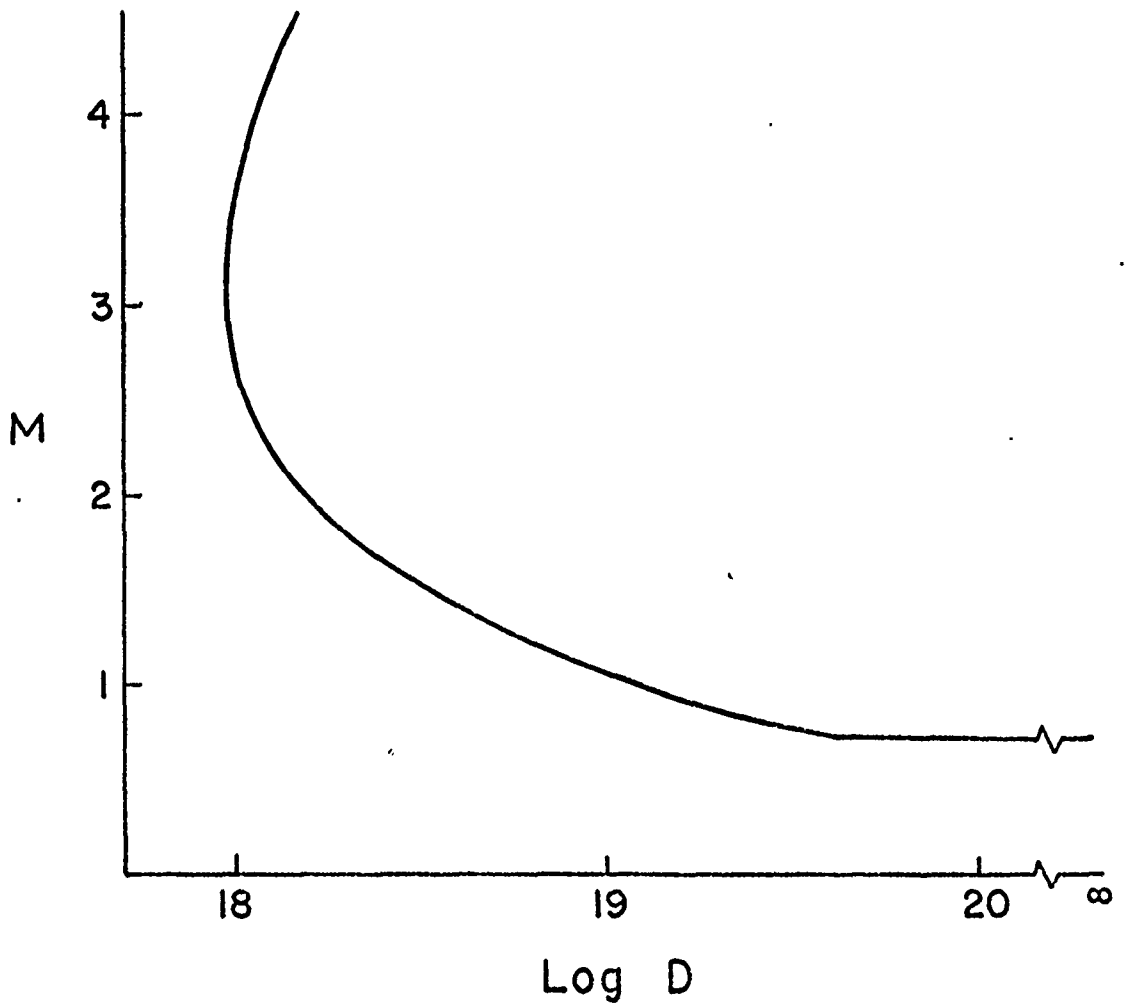

Fig. 6. C-response for $\theta = 50$ and
a) $T_\infty = 1$, $T_s = 1.25$, $L = 0.75$.

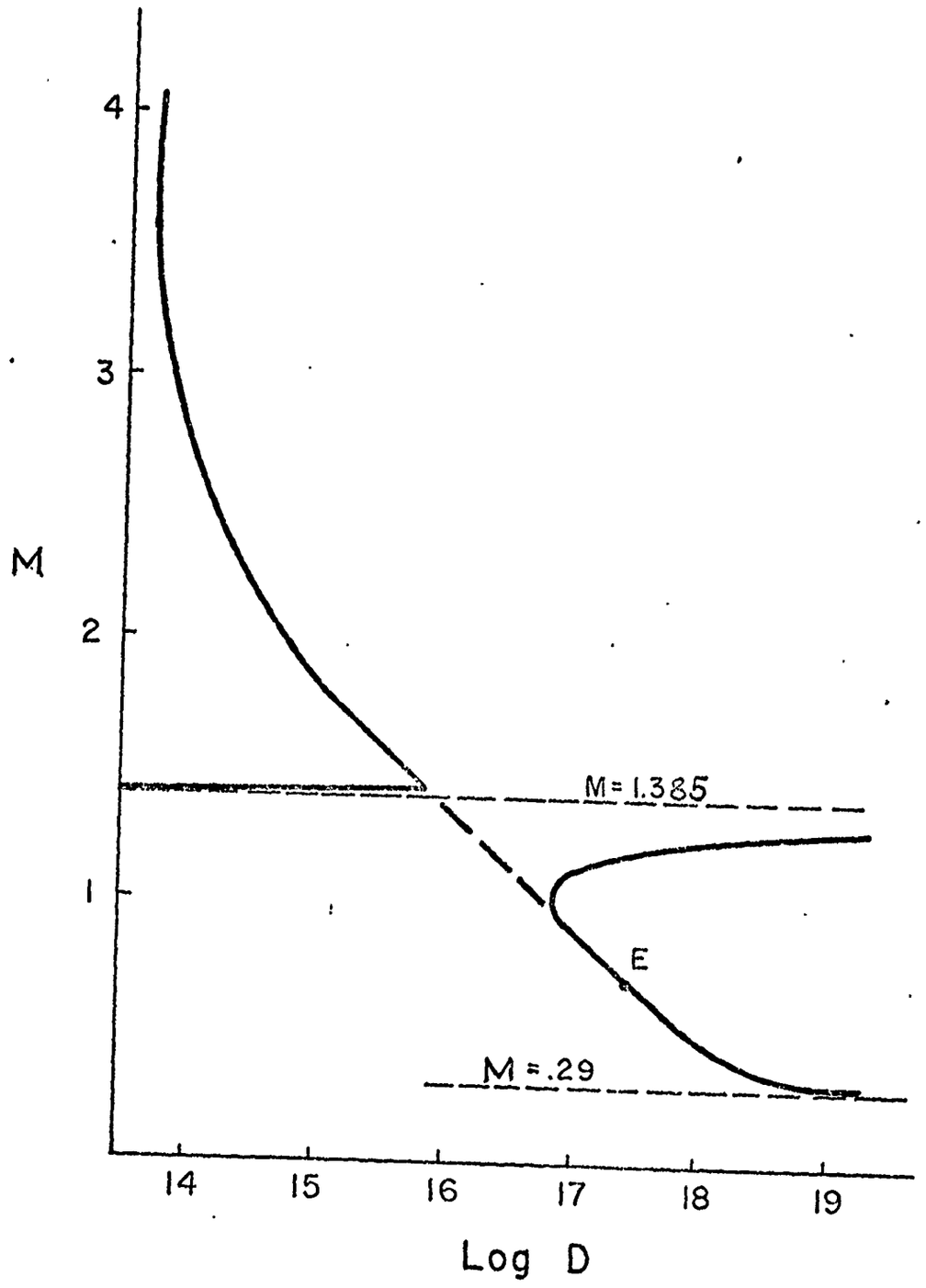

Fig. 6. C-response for $\theta = 50$ and

b) $T_\infty = 1$, $T_s = 1.25$, $L = 0.25$.

SECURITY CLASSIFICATION OF THIS PAGE (When Data Entered)

REPORT DOCUMENTATION PAGE		READ INSTRUCTIONS BEFORE COMPLETING FORM
1. REPORT NUMBER: 109	2. GOVT ACCESSION NO.: AD-A083 546	3. RECIPIENT'S CATALOG NUMBER:
4. TITLE (and Subtitle): MATHEMATICAL THEORY OF LAMINAR COMBUSTION VII Cylindrical and Spherical Premixed Flames		5. TYPE OF REPORT & PERIOD COVERED: Interim Technical Report 6. PERFORMING ORG. REPORT NUMBER:
7. AUTHOR(s): J.D. Buckmaster & G.S.S. Ludford		8. CONTRACT OR GRANT NUMBER(s): DAAG29-79-C-0121
9. PERFORMING ORGANIZATION NAME AND ADDRESS: Dept. of Theoretical and Applied Mechanics Cornell University, Ithaca, NY 14853		10. PROGRAM ELEMENT, PROJECT, TASK AREA & WORK UNIT NUMBERS: P-15882-M
11. CONTROLLING OFFICE NAME AND ADDRESS: U. S. Army Research Office Post Office Box 12211 Research Triangle Park, NC 27709		12. REPORT DATE: March 1980 13. NUMBER OF PAGES: 27
14. MONITORING AGENCY NAME & ADDRESS (if different from Controlling Office)		15. SECURITY CLASS. (of this report): Unclassified 15a. DECLASSIFICATION/DOWNGRADING SCHEDULE: NA

16. DISTRIBUTION STATEMENT (of this Report)

Approved for public release; distribution unlimited.

17. DISTRIBUTION STATEMENT (of the abstract entered in Block 20, if different from Report)

NA

18. SUPPLEMENTARY NOTES

The findings in this report are not to be construed as an official Department of the Army position, unless so designated by other authorized documents.

19. KEY WORDS (Continue on reverse side if necessary and identify by block number)

Cylindrical premixed flames, spherical premixed flames, near-surface, surface, remote, Damköhler-number asymptotics, ignition, extinction, S-response, C-response, monotonic response, monopropellant drop.

20. ABSTRACT (Continue on reverse side if necessary and identify by block number)

This report is Chapter VII of the twelve in a forthcoming research monograph on the mathematical theory of laminar combustion. Cylindrical and spherical premixed flames are discussed, the latter with a view to application to the burning monopropellant drop. Cylindrical flames have a planar character, while spherical flames exhibit ignition and extinction.

DD FORM 1 JAN 73 1473 EDITION OF 1 NOV 65 IS OBSOLETE

Unclassified

SECURITY CLASSIFICATION OF THIS PAGE (When Data Entered)